Article

Design and Construction of Magnetic Coils for Quantum Magnetism Experiments

Graciana Puentes [1,2,3]*

[1] *Departamento de Física, Facultad de Ciencias Exactas y Naturales, Universidad de Buenos Aires, Ciudad Universitaria, 1428 Buenos Aires, Argentina*

[2] *CONICET-Universidad de Buenos Aires, Instituto de Física de Buenos Aires (IFIBA), Ciudad Universitaria, 1428 Buenos Aires, Argentina*

[3] *MIT-CUA, Massachusetts Institute of Technology, Cambridge, Massachusetts 02139, USA.*

* Correspondence: gpuentes@df.uba.ar

Abstract: We report on the design and construction of a spin-flip Zeeman slower, quadrupole magnetic trap and Feshbach field for a new machine for ultra-cold Li-7. The small mass of the Li-7 atom, and the tight lattice spacing, will enable us to achieve a 100-fold increase in tuneling rates over comparable Rb-87 optical lattice emulator experiments. These improvements should enable to access new regimes in quantum magnetic phase transitions and spin dynamics.

Keywords: Cold atoms; Zeeman slower; quadrupole magnetic trap

INTRODUCTION

Quantum Magnetism

In recent years, great development in the simulation of Hubbard and spin models has been observed [Ref1]. Hubbard models of condensed matter systems represent useful approximations for many interesting problems, such as High-Tc superconductivity, frustrated anti-ferromagnetism and spin liquids [Ref2]. Ultra-cold atomic gases confined in an optical lattice allow a practically perfect realization of such models [Ref3], with the advantage over magnetic materials that the parameters may be changed faster, reversibly and more easily. Furthermore, in some limits, Hubbard models reduce to a variety of interesting spin models, which cold atoms and ions can simulate [Ref4]. Specifically, spin-spin interactions can be implemented by controlled collisions [Ref5], on-site interactions [Ref6] and super-exchange interactions [Ref7]. Thus, optical lattice emulators open up a broad avenue for quantum simulations of novel and exotic magnetic materials, and represent a good candidate for performing scalable quantum computations [Ref8].

Li-7 Machine

Li-7 is a particularly suitable species for quantum simulation experiments with ultra-cold atoms, as it presents broad Feshbach resonances at accessible magnetic fields, which can be used as a control parameter for collision properties, and also due to its low mass, which translates into a recoil energy ($E_R=h^2k^2/2m$) orders of magnitude larger than other comparable bosonic species, such as Rb-87 or Na-23. Such higher recoil energies allow for faster tunneling rates, thus enabling the investigation of new regimes in quantum magnetism and spin-dynamics. The Li-7 machine presented in [Ref19] represent an improvement, and a slight simplification, over previous constructions [Ref9], and will be used in the future for optical lattice emulator experiments. One of the main distinction over previous designs for bosonic ultra-cold atoms at MIT is the use of an optically plugged quadrupole magnetic trap. In this review, the different steps towards the design and construction of

the magnetic coils utilized in the 7Li machine are described. **The novelty of the work resides in the construction of an optically plugged quadrupole magnetic trap, the first of its kind at MIT. Moreover, the instrument design and the numerical simulations have been done specifically for Li7 atoms, since Li7 can enable an increase in tunneling rates. There are no former designs, simulations, and measurements for this species in combination with a plugged quadrupole trap.**

In Section I, we present the numerical simulation and experimental results for the (spin-flip) Zeeman slower, where atoms are slowed down by a combination of radiation pressure and Zeeman shift to velocities of a few m/s. In Section II, we present the numerical simulations and experimental results for the construction of a quadrupole magnetic trap which is used to trap the atoms at the main chamber, as they leave the Zeeman slower. In Section III, we present numerical results for Feshbach field. Finally, in Section IV we outline the conclusions. **The results presented in this review are based on numerical simulations, and all numerical simulations are backed up by successful measurements and experimental results. In particular experimental results confirming theoretical prediction for the Zeeman slower are presented in Fig.2 and Fig.3, and the experimental results confirming theoretical prediction for quadrupole magnetic trap are presented in Figs 8. Fig. 9 Fig. 10. Moreover, the magnetic coils described in this report have been successfully utilized in a new machine for ultra-cold atoms as reported in Ref. [19] (PRA Rapid Communications, 2017), which further validates the design and construction of the magnetic coils reported here, and further motivates this publication.**

I.ZEEMAN SLOWER

Doppler Shift and Zeeman Force

We generate a large flux of thermal atoms by a standard effusive atomic beam oven technique [Ref10, Ref11]. The atomic beam leaving the oven has a typical temperature of 450 K (or more), and is collimated enough in order to follow a Boltzmann distribution of longitudinal velocities. We designed the slower for a characteristic (most probable) velocity of around v=960 /s. In order to maximize the flux of particles we want to build a Zeeman slower optimized for a range of velocities around this most probable velocity. Typically this range is 2/3 of the Boltzmann distribution [Ref12]. The atoms are then slowed by means of a laser cooling technique known as Zeeman slowing, which uses a laser counter-propagating to the atomic beam together with a spatially varying magnetic field [Ref13]. As the atoms move with velocity **v** along the slower they see the laser light shifted by an amount proportional to their velocity **v**, due to Doppler shift. The Doppler shift makes the radiation pressure on the atoms dependent on velocity, via the change in the detuning frequency:

$$\delta = \delta_0 - \mathbf{k}.\mathbf{v}, \qquad (1)$$

where $\delta_0 = \omega_{laser} - \omega_{atom}$ is the laser detuning. This means that as the atoms reduce their velocity they get more and more out of tune with the laser frequency (δ increases) and therefore the radiation force gets smaller. A solution to this problem is to introduce a spatially dependent magnetic field B which can shift the atomic transitions and, in turn, compensate for the Doppler detuning. This is the main role of the Zeeman slower, which provides a spatially varying external magnetic field.

For a transition involving a ground state g and excited state e, characterized with magnetic quantum numbers M_g and M_e, and Lande g-factors g_g and g_e respectively, the energy shift introduced by the external B-field is given by:

$$\Delta E = \mu' \mu_B B, \qquad (2)$$

where $\mu' = (g_e M_e - g_g M_g)$, and μ_B is Bohr's magneton. Thus, in order to compensate for the Doppler shift we need $h\delta = \mu' \mu_B B$, which determines a Zeeman field of the form:

$$B(z) = h(\delta_0 - k.v(z)) \quad (3)$$

where we are assuming that v is the longitudinal velocity in the direction of the B-field.

Spin-flip Zeeman Slower

In order to have a large flux atoms to trap we need to slow a significant fraction, typically 2/3 (or more) of the Boltzmann distribution of velocities characterizing the atoms leaving the oven. In the case of a field increasing slower for Li-7, this would require large magnetic fields (i.e., 1000G or more), which can introduce magnetic fringing at the trap position, located close to the end of the slower. A spin-flip slower can be designed in order to reduce the magnitude of the field close to the trap. The main idea is to design a field decreasing (B_{ini}=600G) first section, a zero field (or spin-flip) middle section and a field increasing final section (B_{final}=−400G). By adjusting the laser detuning (600MHz in our case), the initial and final fields it is possible to achieve a field profile with final B-field of only a few hundred G near the vacuum chamber.

Simulations

The main criteria to decide if a Zeeman slower design is good enough is that the difference between the ideal field and the field achieved by winding a set of coils of different radii should be less than the atomic line-width (i.e., 5.9MHz in the case of Li-7 D2 line, which in terms of B-field corresponds to approximately 5G). Next, the acceleration along the slower should remain lower than the maximum Doppler acceleration (a_{max},) [Ref12, Ref13], or in other words the parameter $f = a/a_{max}$ should remain smaller than 1, and fluctuate by less than 20% around the chosen target design parameter ($f = 0.6$ in our case) since large fluctuations in f could produce atom losses.

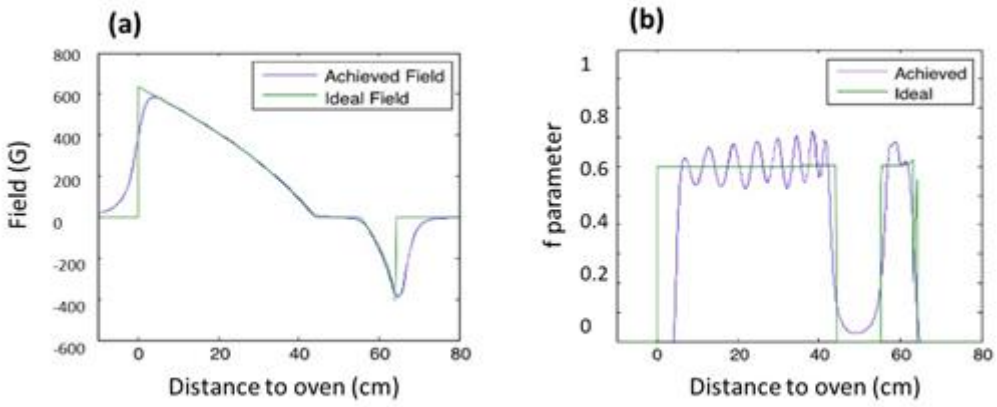

FIG.1. Numerical simulations showing (a) achieved field profile (blue curve), and ideal field profile (green curve), (b) acceleration along the slower, as quantified by the *f* parameter.

The results for our numerical simulation of B-field profile and f-parameter are shown in Fig. 1 (a) and Fig. 1 (b), respectively. As shown in Fig. 1, the design consists of three sections. The first section is the field decreasing part, and requires 11 layers with a number of turns ranging from 116 to 7. The current used for this first Section in the simulations was I = 23Amp. Next there is the B = 0 or spin-flip segment. The length of this segment is eventually determined by length of the bellows. The last section corresponds to the decreasing part of the slower. The first part of this last section consists of a few turns with double spacing (week turns) followed by four layers with and increasing number of turns from 7 to 18. The current used for this second section was I =40A.

Slower measurements

We measured the field by probing the slower with a small current (3 Amps), for each section in series. In order to prevent regions along the slower with this acceleration $a > a_{max}$, we measured the *f* parameter (Fig.2),

and found that at a specific position (z=40cm) *f* had an "unphysical" peak (*f*>1). This peak coincided with the ending of the decreasing section of the slower. We corrected for this by adding one additional turn. Fig.3 show a comparison between the initially measured field (a) and the corrected field (b).

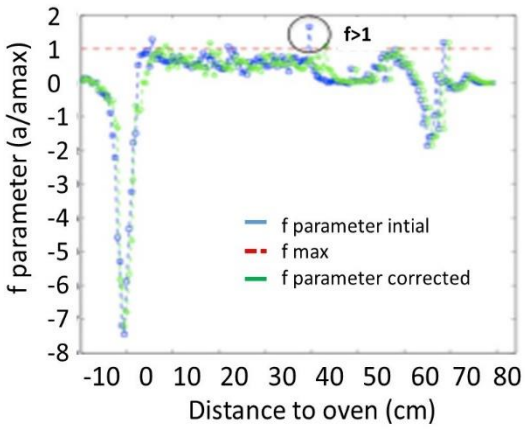

FIG. 2. Measured *f* parameter along the slower. The regions where *f*>1 should be corrected to prevent atom losses.

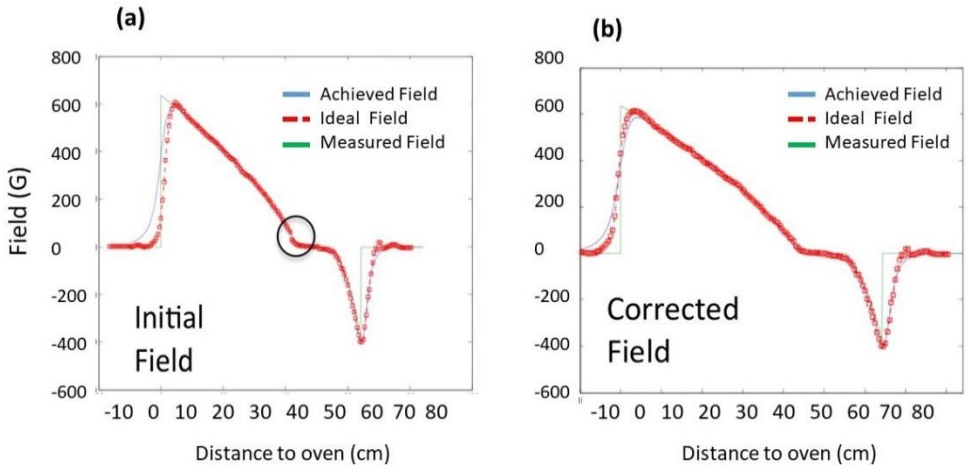

FIG. 3. (a) Initially measured field, (b) corrected field

II. QUADRUPOLE MAGNETIC TRAP

The quadrupole magnetic trap consists of two coils of opposite currents, which produce a magnetic field whose magnitude |B| increases (from zero) with the distance from the center of the trap. The main considerations in designing a quadrupole trap are the separation between coils (Δz), the inner radius of the coils (R) and the number of turns N. In order to fit the coils in our existing bucket windows (see Section IV) the separation should be Δz = 1.5in, and the maximum outer radius should be 6.5in. For thick copper wire (0.1875 in) this corresponds to N = 8,9. Additionally, as we describe below there is a limitation in the number of layers that can be added due to water cooling considerations. Our aim is to cool each layer separately so that each layer can have its own independent current. Taking this into account, 5 layers is approximately the maximum number that we can consider.

The quadrupole trap is easy to construct and gives a tight confinement, but the zero of the magnetic field in the middle of the trap eventually becomes a problem when the cloud is cooled below the temperature where Majorana spin-flips are important. The standard solution is to use a magnetic trap which has a bias field (i.e. the trap bottom has a nonzero magnetic field). In contrast, our approach is to use optical dipole force to

compensate for this, the so called optically plugged quadrupole trap. We note that plugged traps have readily been used, but not in combination with quadrupole magnets.

Non adiabatic spin-flip

As mentioned, one of the limitations of the quadrupole magnetic trap,is that due to the minimum (B = 0) of the field at the center of the traps, atoms with velocity v and mass m can undergo a Majorana transition or non-adiabatic Spin-flips when the Larmor frequency [1,2].

$$\omega_{Larmor} = \mu_B bB'/\hbar < \frac{d\theta_B}{dt} \qquad (9),$$

Loss occurs within a ellipsoid of radius:

$$b_0 = \sqrt{\frac{v\hbar}{\mu_B B'}} \qquad (10).$$

A solution to this problem is to plug the trap hole by using a detuned laser (plug laser), which introduces a optical potential which shifts the atoms (AC Stark shift).

Optical Dipole Force

We can calculate the AC Stark shift due to the plugged laser beam using an expression for the dipole forces [3,4]. For a two-level atom, the optical potential reads:

$$U(\mathbf{r})_{Stark} = \frac{-\hbar\omega_R(\mathbf{r})^2}{4}\left(\frac{1}{\omega_0 - \omega_L} + \frac{1}{\omega_0 + \omega_L}\right) \qquad (11),$$

where ω_0, ω_L, and ω_R are the resonant, laser and Rabi frequency respectively. The Rabi frequency can be written as:

$$2\omega_R^2(\mathbf{r})/\Gamma^2 = I(\mathbf{r})/I_{SAT}, \qquad I_{SAT} = \frac{\hbar\omega_0^3\Gamma}{12\pi c^2} \qquad (14).$$

The main new result we obtained is that by focusing the plug laser to a few μm it is possible to obtain a sufficiently large frequency shift (around 3 MHz), at accessible laser powers (10W) and realistic B-field gradients (500 G/cm). **The main novel result we obtained is that by focussing the laser to a few μm it is possible to obtain a sufficient frequency shift (around 3 MHz), at accessible laser powers (10W) and realistic B-field gradients (500 G/cm). This is displayed in Figure 3b.**

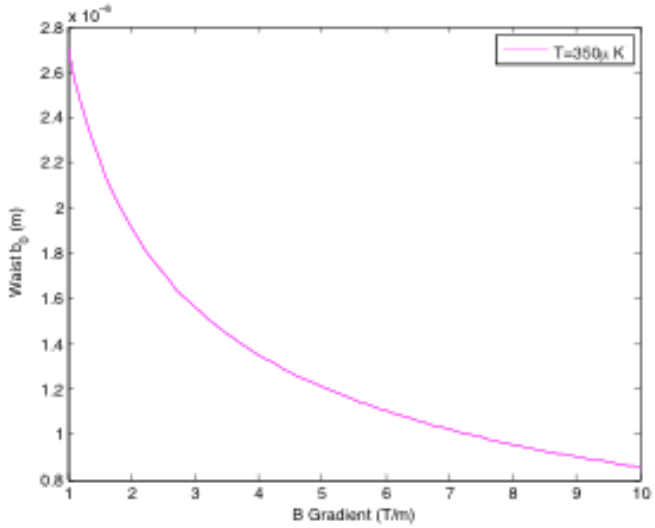

Figure 3b: Waist of Gaussian (plugged) beam for different field gradients.

Field Simulations

The axial magnetic field from a single coil of radius R perpendicular to the z axis, centered at z = A can be written as [Ref. 14]:

$$B_z(r,z) = \frac{\mu_0 I}{2\pi} \frac{1}{[(R+z)^2 + (z-A)^2]^{1/2}} \times E(k^2) \qquad (4)$$

Where $E(k^2)$ is an elliptical integral [1], with $\mu 0 = 4\pi \times 10{-}7$, for vacuum and SI units and $k^2=[4Rr/(R+r)^2+(R-A)^2]$.

Trap Fields

Consider a design consisting of 5 layers, with 9 turns each, and a current of I = 400 Amps in each layer. The axial fields due to each layer (Bz), first and second derivatives (dBz, d_2Bz) are shown in Fig. 4 and Fig.5, respectively.

The field gradient due to each coil individually is around 150G/cm, and can be used independently. Also, these graphs suggest that the total field gradient (i.e. the slope of sum |Bz|) due to the 5 coils is around 750G/cm at 400 Amps (i.e. 1.875G/cmA), while a field gradient of approx. 0.55 G/cmA is required for trapping 7Li, suggesting that our coils should be appropriate for our application.

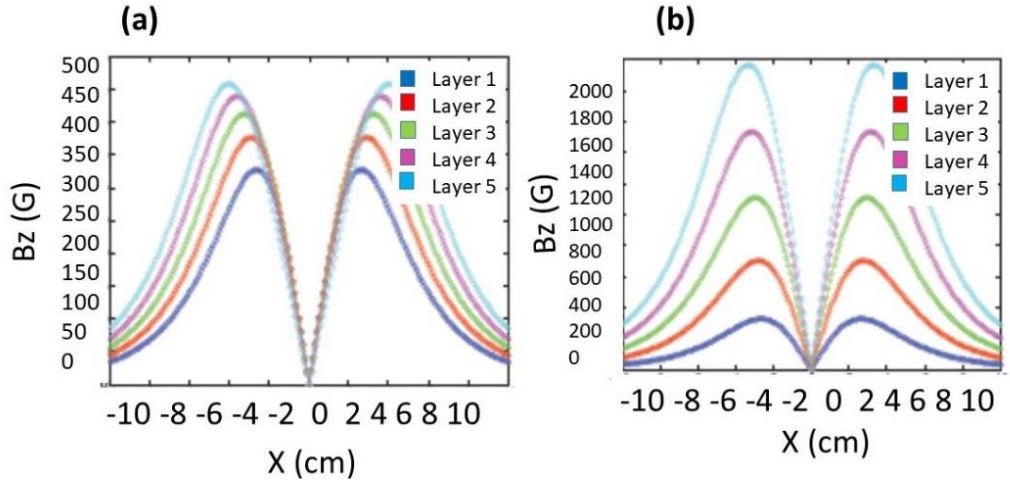

FIG.4. Numerical simulations for (a) |Bz| due to individual layers of a set of coils separated by a distance Dz=0, while running opposite currents (I=400Amps), (b) sum of |Bz| due to each layer.

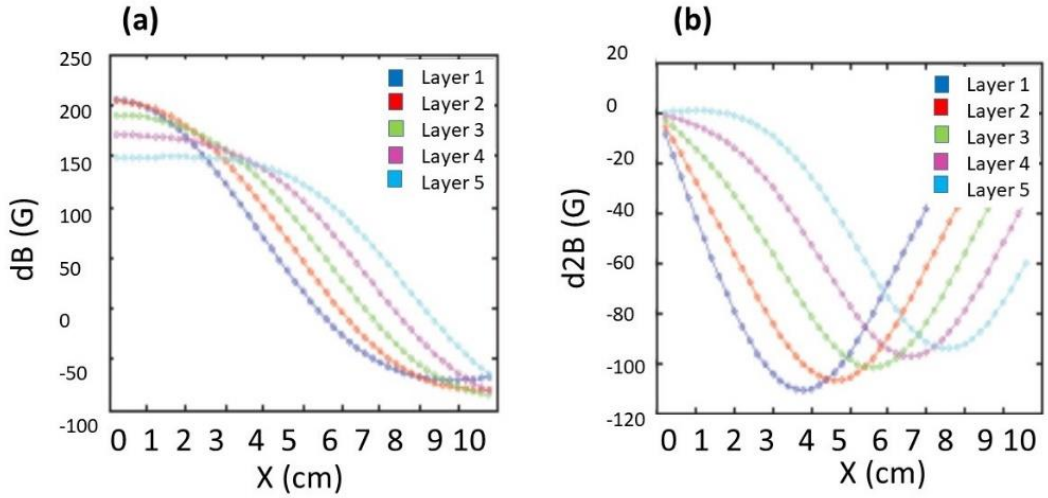

FIG.5. Numerical simulations for: (a) First and (b) second derivative of axial field |Bz| due to individual layers of a set of coils separated by a distance Dz=0 while running opposite currents (I=400Amps).

III. FESHBACH FIELDS

The Feshbach fields are obtained using the same coils but sending both currents in the same direction so that |B| is maximum at the center of the trap. It is also important to have zero curvature ($d_2Bz = 0$) in the Feshbach field at the trap location, for which the layers in the Helmholtz configuration ($R = \Delta z$) will be used. Note that by adding layers 1 and 2 it is possible to achieve fields of up to 900 G, which seems within the range required for tuning the Li-7 resonances. Simulated Feshbach fields are shown on Fig. 6 .

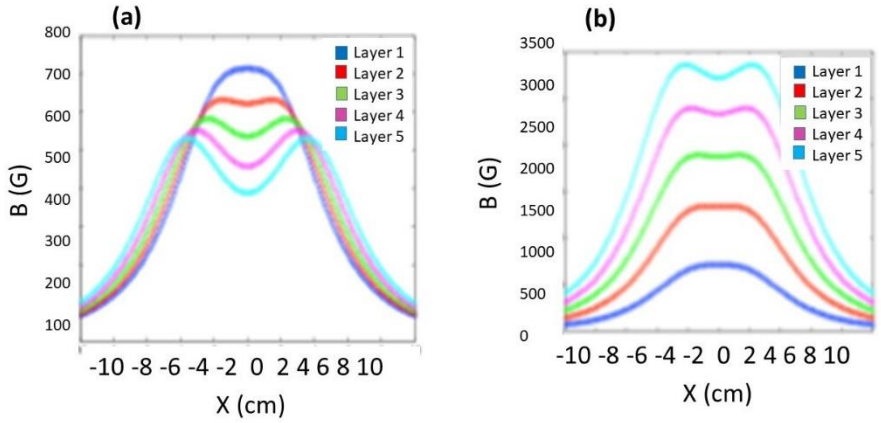

FIG. 6. Numerical simulation of axial field Bz due to (a) individual layers separated by distance Dz=0, (b) sum of field due to individual layers, when running currents equal currents (I=400 Amps).

Fig. 6 shows a simulation of the field that will be used to tune the Feshbach resonances. For this application it is important that the curvature of the field is as small as possible at the position of the trap z = 0. For this purpose layers 1 and 2 should be used, since those are the closest to the Helmholtz configuration. While the plot of the second derivative Fig. 7 (b) shows that this is not exactly zero (about 20G for the innermost layers), this can be corrected using a reverse current in the last layers.

Windings and Measurements

Coil winding can be a very challenging task. One of the main aspects to take into account is that the spacing between coils should be minimum and that the layers should be as 2D as possible. This means that it is necessary to introduce a lot of pressure and tension in the system. Especially during the large amount of time it takes for the Epoxi to cure (6 hours approx).

We measured the fields due to each layer in each coil by sending a small current (5 Amps), and then rescaling it. This is presented in Fig. 8 (a), Fig. 8 (b) shows the corresponding numerical simulation. The error in the field is within 10%, as expected due to small deviations in the shape of coils by bending and additional Epoxi. In order to find the first and second derivates of the measured field at the trap position and then obtain the values for the gradient field and curvature, we fitted the fields with a polynomial expansion [Ref 14]:

$$y = \sum_{n=0} b_n x^n \qquad [5].$$

Once we obtained the fitting coefficients bn we calculated the first and second derivative. Fig. 9 shows the measured (a) and simulated (b) first derivative of the field. Note that while (a) is in inches (b) is in cm. The actual position of the trap in (a) is 0.75in from z=0. From these plots we can see that the first derivative for each layer ranges between 65 G/cm and 80 G/cm, a value which is about 20% smaller than the simulations. We attribute this difference to a propagation of the error in the measured fields. Thus we expect a total field gradient for the quadrupole trap of the order of 600 G/cm.

Fig. 10 (a) Shows the second derivative of the polynomial fit to measured fields, and (b) shows the corresponding simulations. The measured curvatures appear to range between 25 G/cm^2 and 75 G/cm^2. The curvature of the field can eventually be corrected by running a small negative current in the outermost layer.

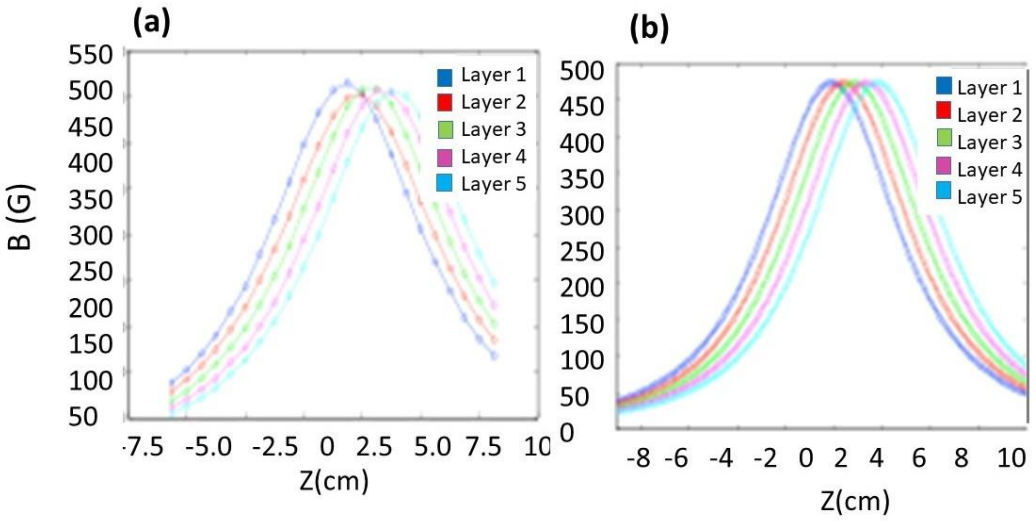

FIG. 8. (a) Measured magnetic field due to a single coil, (b) numerical simulation. The agreement between experiment and theory is apparent.

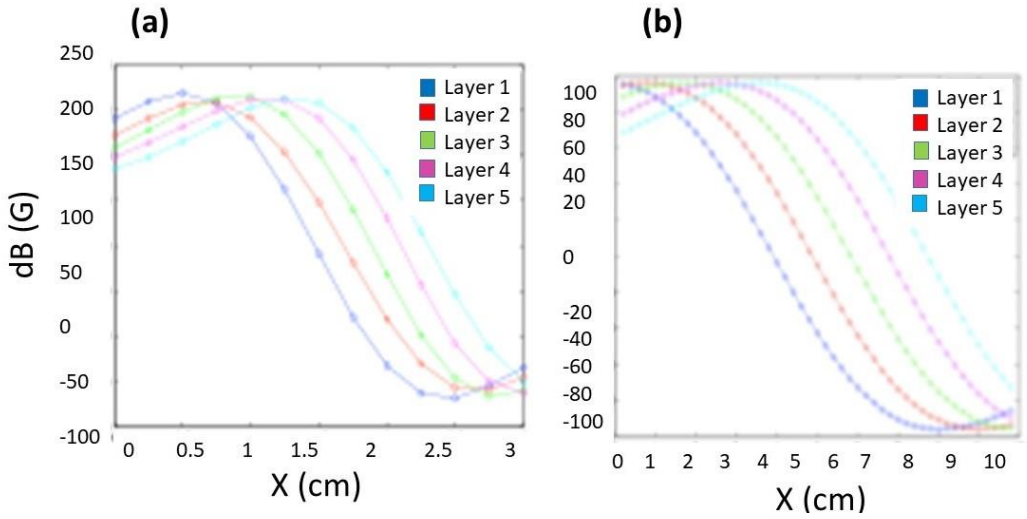

FIG. 9. (a) First derivative of polynomial fit to measured fields, (b) simulation of first derivative.

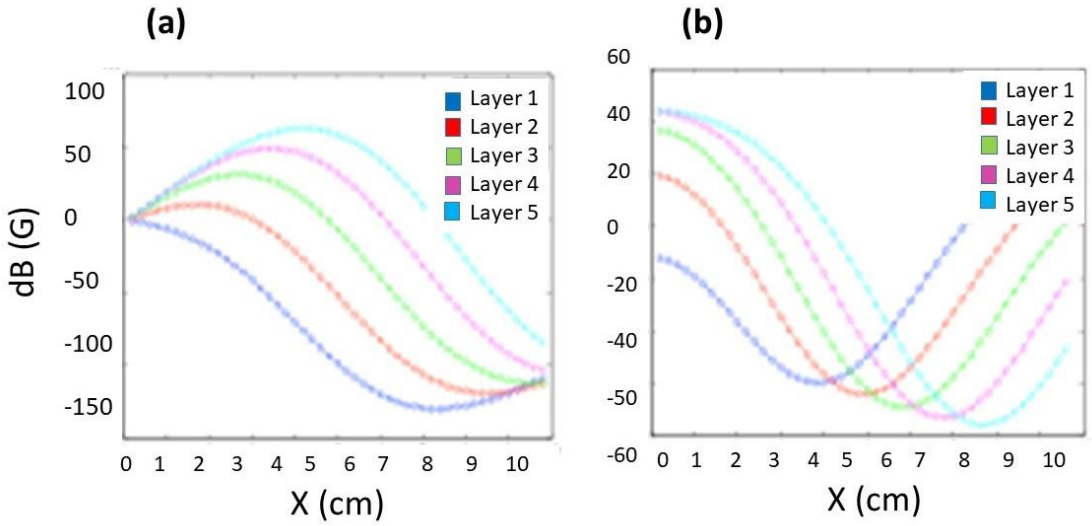

FIG. 10. (a) Second derivative of polynomial fit to measured field, (b) simulation of second derivative.

IV CONCLUSIONS

We presented the design and construction of the magnetic coils for a new machine for ultra-cold Li-7 [19]. In particular, we reported numerical simulations and experimental results for the (spin-flip) Zeeman slower, quadrupole trap, and Feshbach fields. This machine will be employed to emulate novel quantum phases of matter, with ultra-cold Li-7.

ACKNOWLEDGEMENTS

G. Puentes designed and constructed all the components described in this article. The author gratefully acknowledges Wolfgang Ketterle, David Weld, Aviv Keshet, Edward Su, Christian Sanner, Ivana Dimitrova, Niklas Jepsen, and Jesse Amatto-Grill, for useful discussions and technical support.
This work was supported by the NSF through the Center for Ultra-cold Atoms, by NSF award PHY-0969731, through an AFOSR MURI program, and under ARO Grant No.W911NF-07-1-0493 with funds from the DARPA OLE program.

REFERENCES

[1] Ch. Orzel, *Quantum Simulation*, IOP Publishing Ltd 2017
[2] Misguish and Lhuillier, *Frustrated Spin Systems*, World Scientific Singapore (2005); Alet *et al*, Physica A **369**, 122 (2006); Sashdev, Nature Phys. **4**, 173(2008).
[3] Jaksch *et al*, Phys. Rev. Lett. **81**, 3108(1998); Jaksch and Zoller, Ann. Phys. (N. Y.) **315**, 52 (2005).
[4] Dorner *et al*, Phys. Rev. Lett. **91**, 073601(2003); Duan *et al*, Phys. Rev. Lett. **91**,090402 (2003); Garcia-Ripoll, *et al* Phys. Rev. Lett. **93**, 250405 (2004).
[5] Sorensen and Molmer, Phys. Rev. Lett. **83**, 2274 (1999); Mandel et al, Nature **425**, 937 (1999).
[6] Anderlini *et al.*, Nature **448**, 452 (2007).
[7]Trotzky *et al.*, Science **319**, 295 (2008).
[8] Jacks *et al.*, Phys. Rev. Lett. **82**, 1975 (1999).
[9] E. W. Streed *et al.*, Rev. Sci. Instrum. **7**, 023106 (2006).
[10] C.A.Stan, PhD Thesis (2005).
[11] C.A Stan and W. Ketterle, Rev. Sci. Instrum. **76**, 063113 (2005).
[12] C. Foot, *Atomic Physics*, Oxford Univ. Press (2005).
[13] J. Metcalf, *Laser cooling and trapping*, Springer (1999).
[14] T. Bergeman, G. Erez, and H. Metcalf.. Phys. Rev. A **35**, 1535 (1987).
[15]D.Montgomery, *Solenoid Magnet Design*, Wiley-Interscience (1969).

[16] E. W. Streed PhD Thesis (2006).
[17] Davis *et al.*, Phys. Rev. Lett. **75**, 3969 (1995).
[18] Petrich *et al.*, Phys. Rev. Lett. **74**, 3352 (1995).
[19] I. Dimitrova, W. Lunden, J. Amato-Grill, N. Jepsen, Y. Yu, M. Messer, T. Rigaldo, G. Puentes, D. Weld, W. Ketterle, Phys. Rev. A **96**, 051603 (2017).